

# Modified Citrus Pectin Alleviates Cerebral Ischemia/Reperfusion Injury by Inhibiting NLRP3 Inflammasome Activation via TLR4/NF- $\kappa$ B Signaling Pathway in Microglia

Yu Cui<sup>1,2</sup>, Nan-Nan Zhang<sup>1</sup>, Dan Wang<sup>1</sup>, Wei-Hong Meng<sup>2</sup>, Hui-Sheng Chen<sup>1</sup>

<sup>1</sup>Department of Neurology, General Hospital of Northern Theater Command, Shenyang, People's Republic of China; <sup>2</sup>Department of Life Science and Biopharmaceutics, Shenyang Pharmaceutical University, Shenyang, People's Republic of China

Correspondence: Hui-Sheng Chen, Department of Neurology, General Hospital of Northern Theater Command, Shenyang, People's Republic of China, Email [chszh@aliyun.com](mailto:chszh@aliyun.com); Wei-Hong Meng, Department of Life Science and Biopharmaceutics, Shenyang Pharmaceutical University, Shenyang, People's Republic of China, Email [meng.wei hong@qq.com](mailto:meng.wei hong@qq.com)

**Background:** Galectin-3 acts as a mediator of microglial inflammatory response following stroke injury. However, it remains unclear whether inhibiting galectin-3 protects against cerebral ischemia/reperfusion injury. We aimed to investigate the neuroprotective effects of modified citrus pectin (MCP, a galectin-3 blocker) in ischemic stroke and underlying mechanisms.

**Methods:** The middle cerebral artery occlusion/reperfusion (MCAO/R) model in C57BL/6J mice and oxygen-glucose deprivation/reoxygenation (ODG/R) model in neuronal (HT-22) and microglial (BV-2) cells were utilized in the following experiments: 1) the neuroprotective effects of MCP with different concentrations were evaluated in vivo and in vitro through measuring neurological deficit scores, brain water content, infarction volume, cell viability, and cell apoptosis; 2) the mechanisms of its neuroprotection were explored in mice and microglial cells through detecting the expression of NLRP3 (NOD-like receptor 3) inflammasome-related proteins by immunofluorescence staining and Western blotting analyses.

**Results:** Among the tested concentrations, 800 mg/kg/d MCP in mice and 4 g/L MCP in cells, respectively, showed in vivo and in vitro neuroprotective effects on all the tests, compared with vehicle group. First, MCP significantly reduced neurological deficit scores, brain water content and infarction volume, and alleviated cell injury in the cerebral cortex of MCAO/R model. Second, MCP increased cell viability and reduced cell apoptosis in the neuronal ODG/R model. Third, MCP blocked galectin-3 and decreased the expression of TLR4 (Toll-like receptor 4)/NF- $\kappa$ Bp65 (nuclear factor kappa-B)/NLRP3/cleaved-caspase-1/IL-1 $\beta$  (interleukin-1 $\beta$ ) in microglial cells.

**Conclusion:** This is the first report that MCP exerts neuroprotective effects in ischemic stroke through blocking galectin-3, which may be mediated by inhibiting the activation of NLRP3 inflammasome via TLR4/NF- $\kappa$ B signaling pathway in microglia.

**Keywords:** cerebral ischemia/reperfusion injury, microglia, galectin-3, modified citrus pectin, NLRP3 inflammasome

## Introduction

Stroke is the second most common cause of death and major cause of disability worldwide, most of which were ischemic stroke.<sup>1</sup> Although intravenous thrombolysis with recombinant tissue plasminogen activator is the most accessible reperfusion therapy for ischemic stroke, cerebral ischemia/reperfusion injury limits the benefit, which is a severe complication of thrombolytic therapy.<sup>2,3</sup>

Accumulating evidences suggest that microglia-mediated neuroinflammatory responses play critical and complex roles in the ischemia/reperfusion injury.<sup>4-7</sup> Galectin-3, as a pleiotropic endogenous protein, is reported to act as a Toll-like Receptor 4 (TLR4) ligand and promote microglial activation and proliferation in stroke.<sup>8-10</sup> In the activated microglia, NOD-like receptor 3 (NLRP3) inflammasome is subsequently activated to increase the release of inflammatory cytokines,<sup>11</sup> which further deteriorate brain injury in the early phase after ischemic stroke.<sup>12</sup> Modified citrus

pectin (MCP) is known as a blocker of galectin-3 to inhibit its activity through binding to the carbohydrate recognition domains on galectin-3.<sup>13</sup> Recently, in several diseases, MCP was proven to exert anti-inflammatory effect by blocking galectin-3.<sup>14–17</sup> Furthermore, higher plasma galectin-3 levels were found to be associated with poor functional outcomes after acute ischemic stroke.<sup>18–23</sup> Collectively, cerebral ischemic insult may promote the expression of galectin-3 in microglia, and then trigger the activation of NLRP3 inflammasome in microglia through TLR4/NF- $\kappa$ B signaling pathway, which converts caspase-1 into cleaved-caspase-1. In this context, we argue that blocking galectin-3 by MCP will exert neuroprotective effect in ischemic stroke. However, up to date, no studies have been found to investigate the issue.

In the present study, we first used *in vivo* experiments to evaluate whether MCP prevented cerebral ischemia/reperfusion injury by blocking galectin-3 on microglia. Then, *in vitro* experiments were used to evaluate whether MCP produced neuroprotective effects on neurons through microglia. Lastly, *in vivo* and *in vitro* experiments were used to explore the possible mechanisms underlying the neuroprotection of MCP in cerebral ischemia/reperfusion injury.

## Materials and Methods

The experimental procedure and study timeline are shown in [Figure 1A](#).

### Animals and Experimental Groups

The article adheres to the ARRIVE (Animals in Research: Reporting In Vivo Experiments) guidelines for reporting *in vivo* experiments 2.0 and reporting standards for preclinical studies ([Supplementary Table 1](#)).<sup>24,25</sup> C57BL/6J male adult mice (age, 10–12 weeks; weight, 25–30 g; from the Liaoning Changsheng Biotechnology Company Limited, Shenyang, Liaoning, China) were used in the experiments. Given the effect of gender on stroke prognosis, only male mice were selected for this study. The mice were housed specific pathogen-free conditions at a 12/12-hour light/dark cycle with free access to water and food during the experiment. Data collection and analyses were performed by a researcher blinded with respect to the treatment group.

In the *in vivo* experiment, a total of 81 mice were used and randomly divided into 5 groups: (1) sham + vehicle ( $n = 9$ ); (2) middle cerebral artery occlusion/reperfusion (MCAO/R) + vehicle ( $n = 18$ ); (3) MCAO/R + 200 mg/kg/d MCP ( $n = 18$ ); (4) MCAO/R + 400 mg/kg/d MCP ( $n = 18$ ); (5) MCAO/R + 800 mg/kg/d MCP ( $n = 18$ ). All mice were included except the following exclusions: 12 mice failed to establish model because of hemorrhage or no neurological deficits (neurological deficit scoring  $<2$ ) after reperfusion, and 24 mice died after ischemia induction ([Supplementary Table 2](#)). The remaining 45 mice were sacrificed at 1 day after MCAO/R operation and used for neurological function tests, measurement of infarct size and brain water content, and TUNEL (Terminal-deoxynucleotidyl Transferase Mediated Nick End Labeling), FJB (Fluoro-Jade B), and immunofluorescence staining, and Western blot analysis ([Figure 1B](#)).

### MCAO/R Modeling

The MCAO/R model operation was performed as previously described.<sup>26</sup> Briefly, the mice were first anesthetized with 1% sodium pentobarbital (30 mg/kg) by intraperitoneal injection. Then, an incision was made in the skin and the right common carotid artery, external carotid artery, and internal carotid artery were carefully exposed. A nylon 6–0 filament was inserted into the stump of external carotid artery and advanced into the internal carotid artery until it was advanced at a predetermined distance of 8 mm from the carotid bifurcation to the middle cerebral artery. After a 1 hour period of focal cerebral ischemia, the filament was gently removed (reperfusion onset). The collar suture at the base of the external carotid artery stump was then tightened. The skin incision was closed. The sham-operation mice underwent neck dissection and coagulation of the external carotid artery, but the middle cerebral artery was not occluded. The mice body temperature was monitored and stabilized at  $37\pm 0.5^{\circ}\text{C}$  under a homeothermic heating pad.

### Drug Treatment

MCP (Centrax International Corporation, San Francisco, USA) was dissolved with 0.9% sterile saline to desired concentrations. The initial MCP concentration of 200 mg/kg/d for C57BL/6J mice was selected according to the conversion of the concentrations for Sprague-Dawley rats in the previous study.<sup>15</sup> Different concentrations of MCP

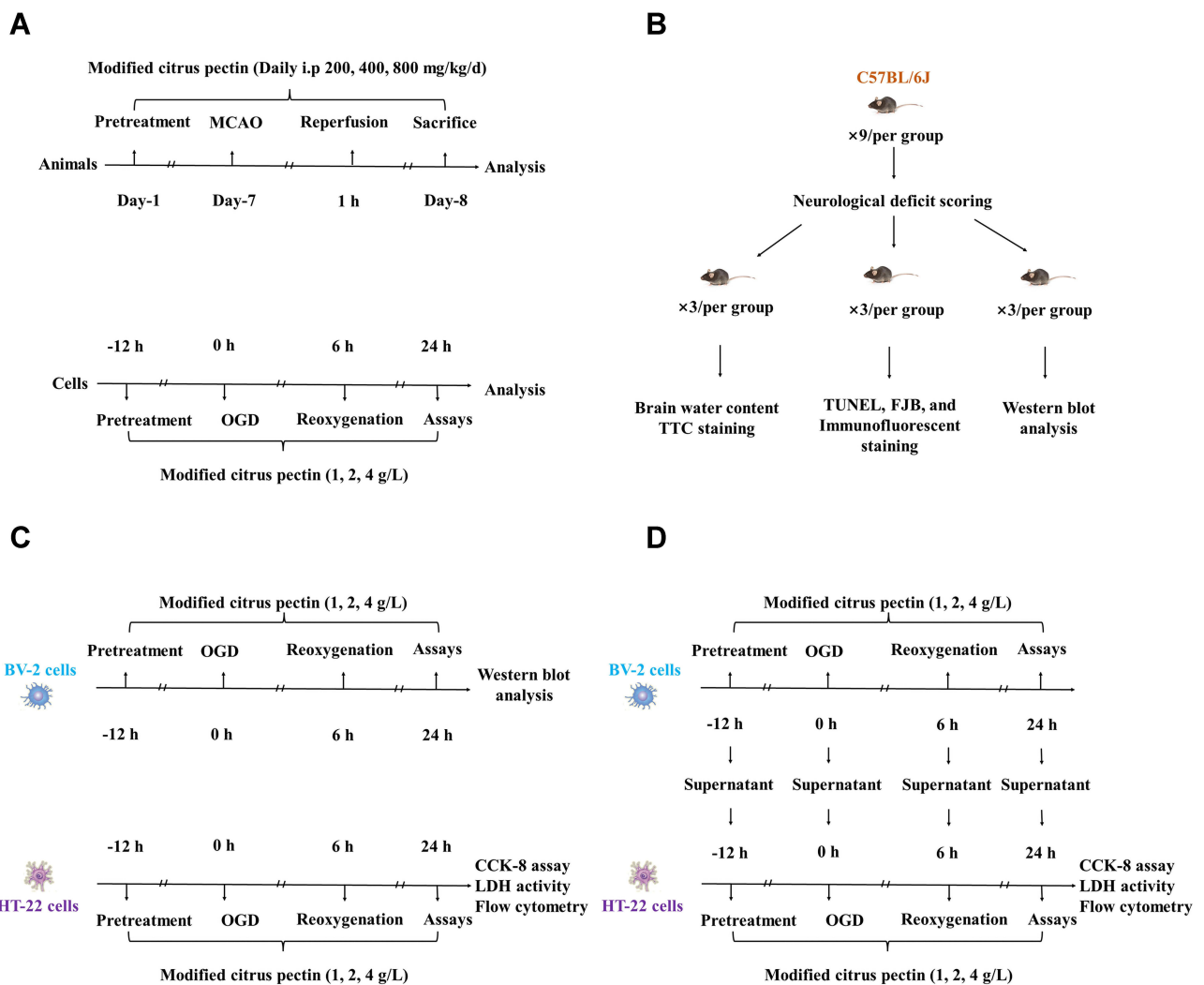


**Figure 1** Experimental protocol of in vivo and in vitro experiments. **(A)** Time profiling of in vivo and in vitro experiments; **(B)** Number of experimental animal in each test group; **(C)** Different tests for HT-22 cells and BV-2 cells after administrated with 1 g/L, 2 g/L, and 4 g/L modified citrus pectin; **(D)** The co-culture design of HT-22 cells with the supernatant of BV-2 cells. CCK-8 indicates cell counting kit 8; FJB, Fluoro-jade B; LDH, lactate dehydrogenase; MCAO, middle cerebral artery occlusion; OGD, oxygen-glucose deprivation; TTC, 2,3,5-triphenyltetrazolium chloride; TUNEL, terminal-deoxynucleotidyl transferase mediated nick end labeling.

(200 mg/kg/d, 400 mg/kg/d, and 800 mg/kg/d) were intraperitoneally administered to mice from 7 days before MCAO operation to 1 day after reperfusion when mice were sacrificed, which was based on our preliminary results ([Supplementary Tables 3 and 4](#), [Supplementary Figures 1 and 2](#)). The sterile saline was administrated as vehicle control.

## Neurological Function Tests

At 1 day after the MCAO operation, mice were tested for neurological deficits by two trained investigators under blinded conditions. The behavioral score was calculated as the mean value of two investigators. A previously published scoring system of 0 to 4 points was adopted as follows: 0, no neurological deficit; 1, the front paw on the paralyzed side cannot be fully extended; 2, circling to the paralyzed side while walking; 3, falling to the paralyzed side while walking; 4, cannot walk automatically or lose consciousness.<sup>27</sup>

## Infarct Size Measurement

Mice were sacrificed through cervical dislocation in the condition of pentobarbital anesthesia. Brain of mice were collected and then refrigerated at  $-20^{\circ}\text{C}$  for 20 minutes. Brain matrix of each mice was cut into 5 slices, soaked in the 2%

2,3,5-triphenyltetrazolium chloride (TTC, G3005, Solarbio, China) at 37°C for 20 min, fixed in the 10% formalin solution, and photographed with camera. Infarction sizes were measured by Image J (version 1.52). The brain edema interference was adjusted (contralateral area – ipsilateral nonischemic area) and relative infarction sizes were performed as percentage of infarction size/prosencephalon size.

## Brain Water Content Measurement

The measurement of brain water content was designed to reflect the degree of cerebral edema secondary to the cerebral ischemia/reperfusion injury. Brain water content was assessed by the wet/dry method at 1 day after reperfusion, as previously described.<sup>28</sup> Briefly, the brains were removed without perfusion, and then wet weights were measured through an electronic balance. After the specimens were heated at 105°C for 24 hours, dry weights were measured. The brain water content was calculated by (wet weight-dry weight)/wet weight × 100%.

## Immunofluorescence Staining

The ischemic penumbra of cerebral cortex is detected in the MCAO/R and MCAO/R+MCP groups, while the cerebral cortex is detected in the Sham group. Firstly, after antigen retrieval, the sections were fixed, permeabilized, and incubated with primary antibodies Iba1 (1:200, ab178847, Abcam, UK), Galectin-3 (1:100, 60207-1-Ig, Proteintech, China), NLRP3 (1:100, MA5-23919, Invitrogen, China). Secondly, the sections were incubated with a Cy3-conjugated (1:200, A27039, Invitrogen, China), or FITC-conjugated (1:100, Ab6785, Abcam, UK) secondary antibody. Finally, diamidino-2-phenylindole (DAPI) was added to stain the nuclei. All the stained sections were viewed by microscope (BX53, Olympus, Japan) and photographed by microscope photographic system (DP73, Olympus, Japan). Density of double-labeled cells was reported as the average number of double labeled cells per square millimeter in each group.

## TUNEL and FJB Staining

Animals were anesthetized and perfused with phosphate buffer saline (PBS) followed by 4% paraformaldehyde, and brains were sectioned into 5-mm-thick frozen slices. The ischemic penumbra of cerebral cortex is detected in the MCAO/R and MCAO/R+MCP groups, while the cerebral cortex is detected in the Sham group. TUNEL staining was performed to detect cell apoptosis by kit (WLA127a, Wanleibio, China). FJB staining was performed to detect cell degeneration by kit (TR-150-FJB, Biosensis, China). Both TUNEL and FJB staining were performed according to the manufacturers' protocols. The stained sections were photographed under a confocal fluorescence microscope (BX53, Olympus, Japan). The nuclei were stained with DAPI positive (blue), apoptotic cells were TUNEL positive (red), and degenerated cells were FJB positive (green). We calculated the number of DAPI positive cells (blue) and TUNEL positive cells (red), and the number of FJB positive cells (green). Four quadrants were selected from each section, number of positive cells in which was counted and calculated on average.

## Cells and Experimental Groups

Cell lines of mouse hippocampal (HT-22, iCell-m020) and murine microglia (BV-2, iCell-m011) were obtained from iCell Bioscience Inc (Shanghai, China), and cultured in Dulbecco's modified Eagle's medium (DMEM, G4510, Servicebio, China) supplemented with 10% fetal bovine serum (FBS, #11011-6125, Zhejiang Tianhang Biotechnology, Co., Ltd., Zhejiang, China) in an incubator (HF-90, Shanghai Lishen Co., Ltd, Shanghai, China) with 5% CO<sub>2</sub> at 37°C. The cultured cells in the logarithmic growth phase were rinsed twice with PBS (B548117, Sangon Biotech, China) and maintained in glucose-free DMEM (PM150270, Procell, China).

In the *in vitro* experiment, BV-2 cells and HT-22 cells were randomly divided into several parts as follows: BV-2 cells, HT-22 cells, and HT-22 cells with supernatant from every stage of BV-2 cells. Each part consisted of 5 groups: (1) Control group: cells were maintained in the normal medium; (2) Oxygen-Glucose Deprivation/Reperfusion (OGD/R) group: cells were insulted by OGD/R; (3) OGD/R + 1 g/L MCP; (4) OGD/R + 2 g/L MCP; (5) OGD/R + 4 g/L MCP. Different concentrations of MCP were added into mediums at 12 hours before OGD/R. The suitable concentrations of MCP were chosen based on our preliminary study ([Supplementary Table 5](#) and [Supplementary Figure 3](#)). The procedure details are shown in [Figure 1C](#) and [1D](#).

## OGD/R Modeling

The HT-22 and BV-2 cells were, respectively, placed into a hypoxic incubator (HF-100, Shanghai Lishen Co., Ltd, Shanghai, China) with 5% CO<sub>2</sub> and 95% N<sub>2</sub> for 6 hours at 37°C to mimic OGD injury. Cultures were then restored with glucose at DMEM and recovered at normoxic conditions (37°C, 5% CO<sub>2</sub>) for 24 hours (OGD restoration).<sup>26</sup> Meanwhile, the supernatant of BV-2 cells were collected after the OGD/R operation. The OGD 6h was selected according to preset test ([Supplementary Table 6](#) and [Supplementary Figure 4](#)) and previous study.<sup>7</sup>

## Cell Viability Assay

Cell Counting Kit (CCK)-8 assay (WLA074b, Wanleibio, China) was used to detect the cell viability. Briefly, HT-22 cell lines were seeded in 96-well plates with DMEM containing 10% FBS. Cells were treated with different concentrations (1 g/L, 2 g/L, and 4 g/L) of MCP from the beginning of OGD until 24 hours. The medium was then removed, and 10 mL of CCK-8 solution was subsequently added to each well. After 2 hours of incubation at 37°C, the absorbance at 450 nm was measured using an automatic microplate reader (800Ts, BIOTEK, USA).

## LDH Activity Assay

After OGD/R operation and MCP administration, HT-22 cell supernatant was moved to 96-well plate. According to manufacturer's protocols of a microplate reader (ELX-800, BIOTEK, USA), cell injury was assessed through detecting lactate dehydrogenase (LDH) level by kit (WLA072, Wanleibio, China) at 450 nm.

## Flow Cytometry

The medium of HT-22 cell was removed after OGD/R operation and MCP administrations, and pooled with adherent cells.<sup>29</sup> Firstly, the mixture was rotated at 150 g for 3 min. Secondly, cells were washed and resuspended in cold PBS, whose density was adjusted to 10<sup>6</sup> cells per well. Lastly, cells were added with 5 μL of Annexin V-FITC and 10 μL of Propidium Iodide, and incubated at room temperature in the dark for 15 min. Cells were subjected to flow cytometry (NovoCyte, Aceabio, USA).

## Western Blot Analysis

Firstly, BCA assay kit (WLA004, Wanleibio, China) and different concentrations of SDS-PAGE gels (WLA013, Wanleibio, China) were used to quantify the proteins in the brain homogenates or BV-2 cell lysates, which were then transferred to PVDF membranes (IPVH00010, Millipore, USA). Secondly, membranes were blocked with 5% non-fat dry milk (Q/NYLB 0039S, Yili, China) in TBST (T1081, Solarbio, China) and incubated with primary antibodies against galectin-3 (1:500, 60207-1-Ig, Proteintech, China), toll-like receptor 4 (TLR4, 1:400, WL00196, Wanleibio, China), nuclear factor kappa-B (NF-κBp65, 1:500, WL01980, Wanleibio, China), caspase-1 (1:500, WL03450, Wanleibio, China), interleukin-1β (IL-1β, 1:1000, WL00891, Wanleibio, China), NLRP3 (1:1000, MA5-23919, Thermo Fisher, USA), and β-actin (1:400, WL01372, Wanleibio, China), and then washed with TBST and incubated with HRP-IgG (1:5000, goat anti-rabbit, WLA023, Wanleibio, China). Lastly, ECL kit (WLA003, Wanleibio, China) was used to detect immunoreactive bands, and Gel-Pro-Analyzer software (WD-9413B, Beijing Liuyi, China) was used to scan and analyze bands. β-actin was set as internal standard to normalize film signals, and signals of sample in Control group were normalized to 1.0.

## Statistical Analysis

Data are presented as mean ± standard deviation (SD). Differences among groups were compared with one-way ANOVA analysis, followed by post-hoc comparison. SPSS statistical software (IBM Version 23) was used for analyzing the obtained data. Statistical significance was set at *p* value <0.05.

## Results

### MCP Showed Neuroprotective Effect in MCAO/R Model

In order to investigate the neuroprotective effect of MCP, neurologic deficit scoring, brain water content, and infarct size were evaluated in mice MCAO/R model. Compared with vehicle, MCP (400 mg/kg/d and 800 mg/kg/d) significantly reduced neurologic deficit scoring ( $p = 0.003$  and  $p < 0.001$ , Figure 2A). Similarly, compared with vehicle, MCP (200 mg/kg/d, 400 mg/kg/d, and 800 mg/kg/d) also significantly reduced brain water content ( $p = 0.02$ ,  $p = 0.011$ , and  $p = 0.002$ , Figure 2B) and infarct size ( $p = 0.003$ ,  $p < 0.001$ , and  $p < 0.001$ , Figure 2C and 2D). Furthermore, MCP (200 mg/kg/d, 400 mg/kg/d, and 800 mg/kg/d) treatment significantly reduced the numbers of TUNEL positive ( $p < 0.001$ ,  $p < 0.001$ , and  $p < 0.001$ , Figure 3A and 3B) and FJB positive cells, compared with vehicle group ( $p < 0.001$ ,  $p < 0.001$ , and  $p < 0.001$ , Figure 3A and 3C). The numerical data are shown in the [Supplementary Tables 7 and 8](#).

### MCP Showed Neuroprotective Effect in OGD/R Model

Given that CCK-8 cytotoxicity and LDH activities could indicate the extent of cell injury and flow cytometry could indicate the extent of cell apoptosis, we performed CCK-8 cytotoxicity, LDH activities, and flow cytometry assay to detect neuroprotective effects of MCP after OGD/R operation. In the CCK-8 cytotoxicity assay, after HT-22 cells were

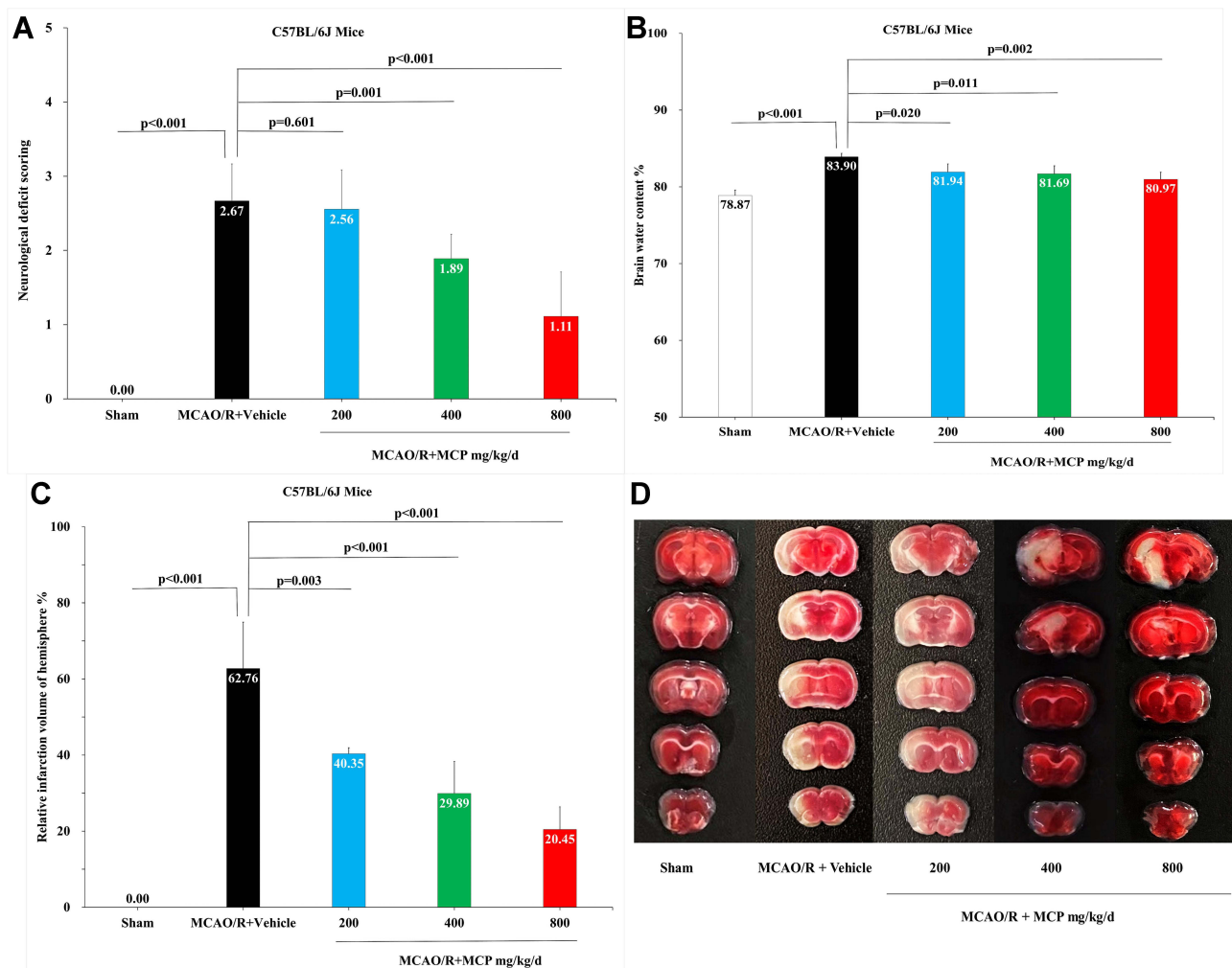


**Figure 2** MCP treatment protected against cerebral ischemia/reperfusion injury in C57BL/6J mice at 1 day after MCAO/R operation. (A) Neurological deficit score test,  $n=9$  per group; (B) Brain water content measurement,  $n=3$  per group; (C) Cerebral infarction size measurement,  $n=3$  per group; (D) Representative TTC (2,3,5-triphenyltetrazolium chloride) staining images,  $n=3$  per group. MCAO/R indicates middle cerebral artery occlusion/reperfusion; MCP, modified citrus pectin. Data are mean  $\pm$  standard deviation.

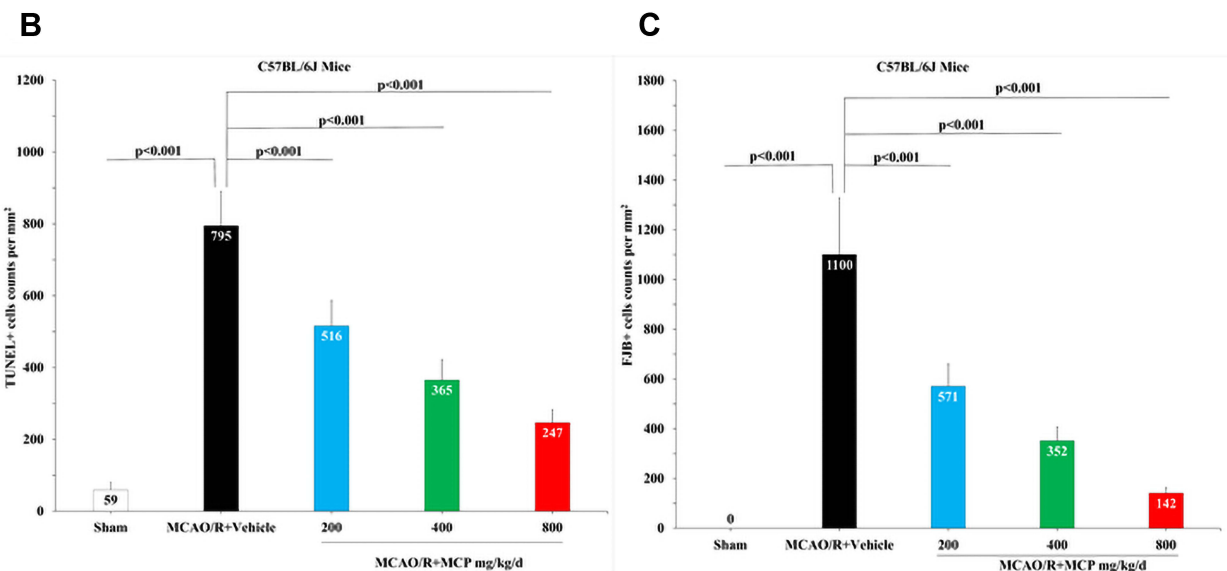
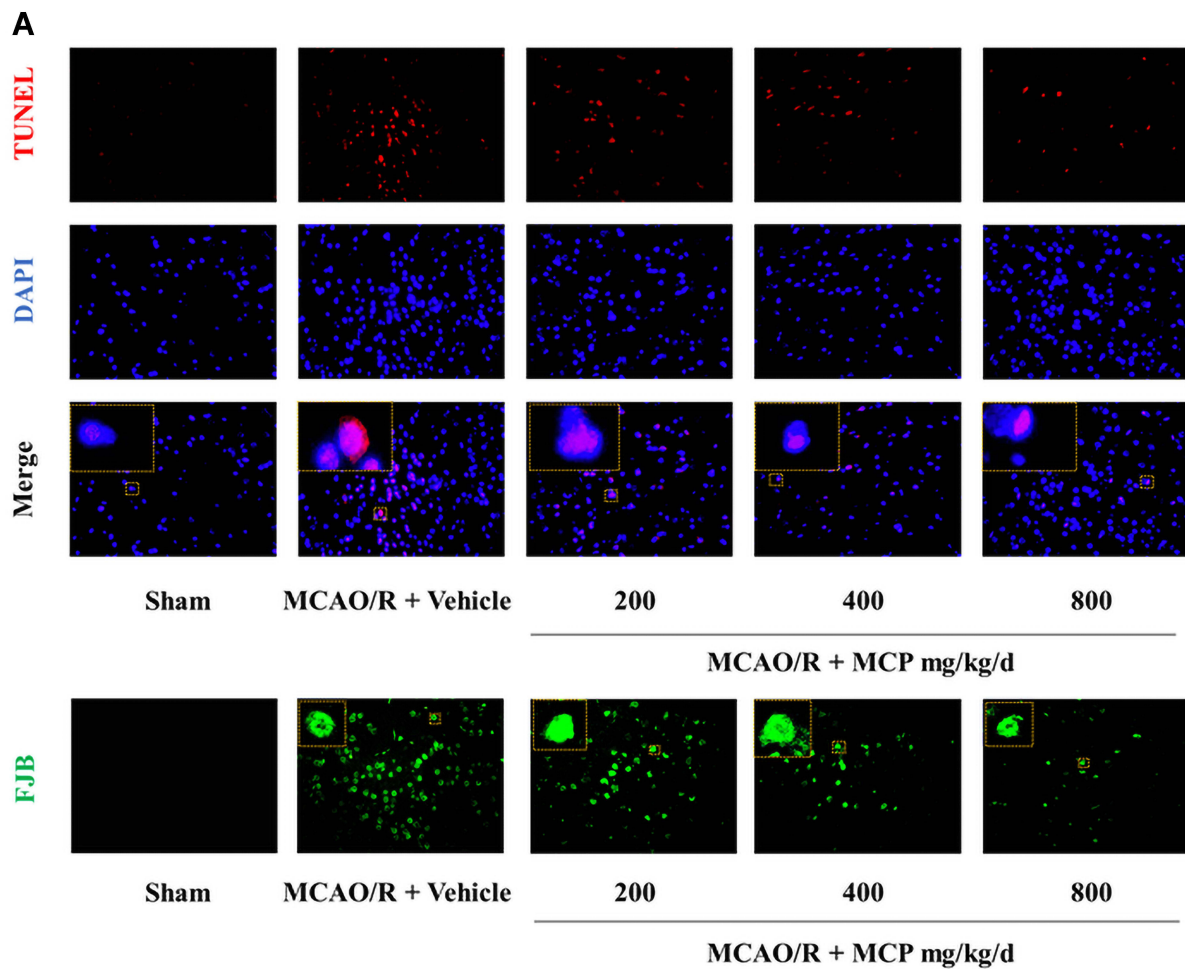


**Figure 3** MCP attenuated neuronal injury and apoptosis in C57BL/6J mice at 1 day after MCAO/R operation. **(A)** Representative TUNEL (Terminal-deoxynucleotidyl Transferase Mediated Nick End Labeling) staining images of cerebral apoptotic cells, counterstained with DAPI and Representative FJB (Fluoro-Jade B) staining images of cerebral injured cells, n=3 per group, scale bar: 50µm. **(B)** Quantification of merged cells in the ischemic penumbra of cerebral cortex. **(C)** Quantification of merged cells in the ischemic penumbra of cerebral cortex. MCAO/R indicates middle cerebral artery occlusion/reperfusion; MCP, modified citrus pectin. Data are mean ± standard deviation.

subjected to OGD/R, cell viability was markedly reduced, which was not changed by MCP administration (Figure 4A). After HT-22 cells co-cultured with BV-2 cell supernatant were subjected to OGD/R, cell viability was also markedly reduced, which was improved significantly after MCP (2 g/L and 4 g/L) administration ( $p = 0.046$  and  $p = 0.001$ , Figure 4B). In the LDH activity assay, after HT-22 alone or co-cultured with BV-2 cell supernatant was subjected to OGD/R, LDH activities of HT-22 cells were significantly increased, while MCP (2 g/L and 4 g/L) administration significantly reduced the increase ( $p < 0.001$  and  $p < 0.001$ , Figure 4C and 4D). Flow cytometry assay showed that neurons apoptosis was increased significantly after OGD/R in HT-22 cells alone or co-cultured with BV-2 cell supernatant, which was effectively reversed after MCP (1 g/L, 2 g/L, and 4 g/L) administration ( $p = 0.001$ ,  $p < 0.001$ , and  $p < 0.001$ , Figure 5). The numerical data are shown in the [Supplementary Tables 9](#) and [10](#). The results suggested that MCP produced neuroprotective effects after OGD/R operation.

## MCP Reduced the Expression of NLRP3, Cleaved-Caspase-1, and IL-1 $\beta$

To investigate whether MCP inhibits neuroinflammation in the cerebral ischemia/reperfusion injury, we detected the expression of NLRP3 inflammasome-associated proteins, including NLRP3, caspase-1, cleaved caspase-1 and IL-1 $\beta$ , in the brain by immunofluorescence staining and Western blotting analyses. NLRP3<sup>+</sup> cell counts showed that cerebral ischemia

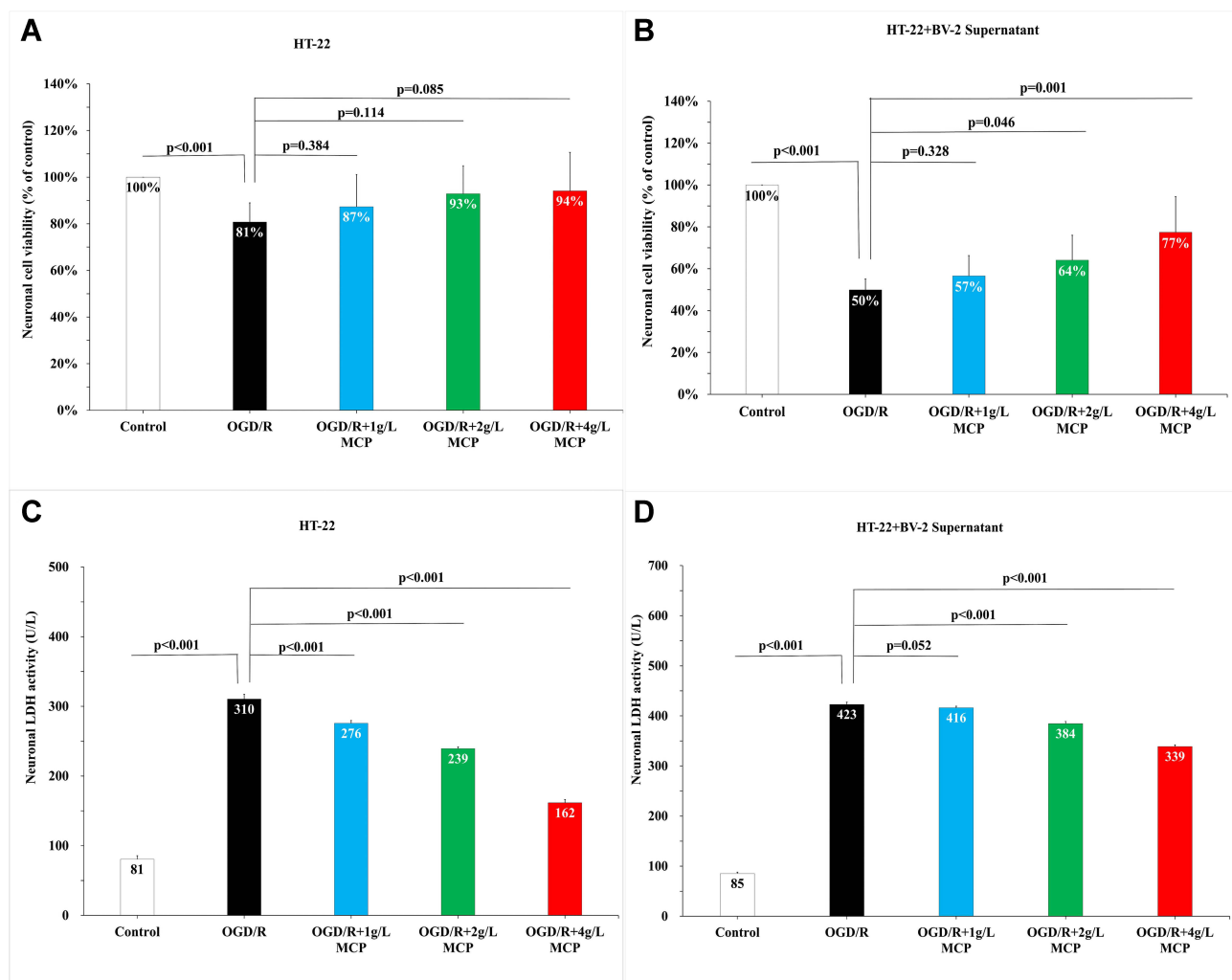


**Figure 4** MCP attenuated neuronal cell viability and injury in OGD/R model. **(A)** Neuronal cell (HT-22) viability after OGD/R was assessed by CCK-8 tests. **(B)** Neuronal cell (HT-22) viability after OGD/R was assessed by CCK-8 tests, when co-cultured with supernatant of BV-2 cells. **(C)** Neuronal cell (HT-22) injury after OGD/R was assessed by LDH activity. **(D)** Neuronal cell (HT-22) viability after OGD/R was assessed by LDH activity, when co-cultured with supernatant of BV-2 cells. MCP indicates modified citrus pectin, OGD/R, oxygen-glucose deprivation/reperfusion. Data are mean  $\pm$  standard deviation, and  $n=5$  per group.



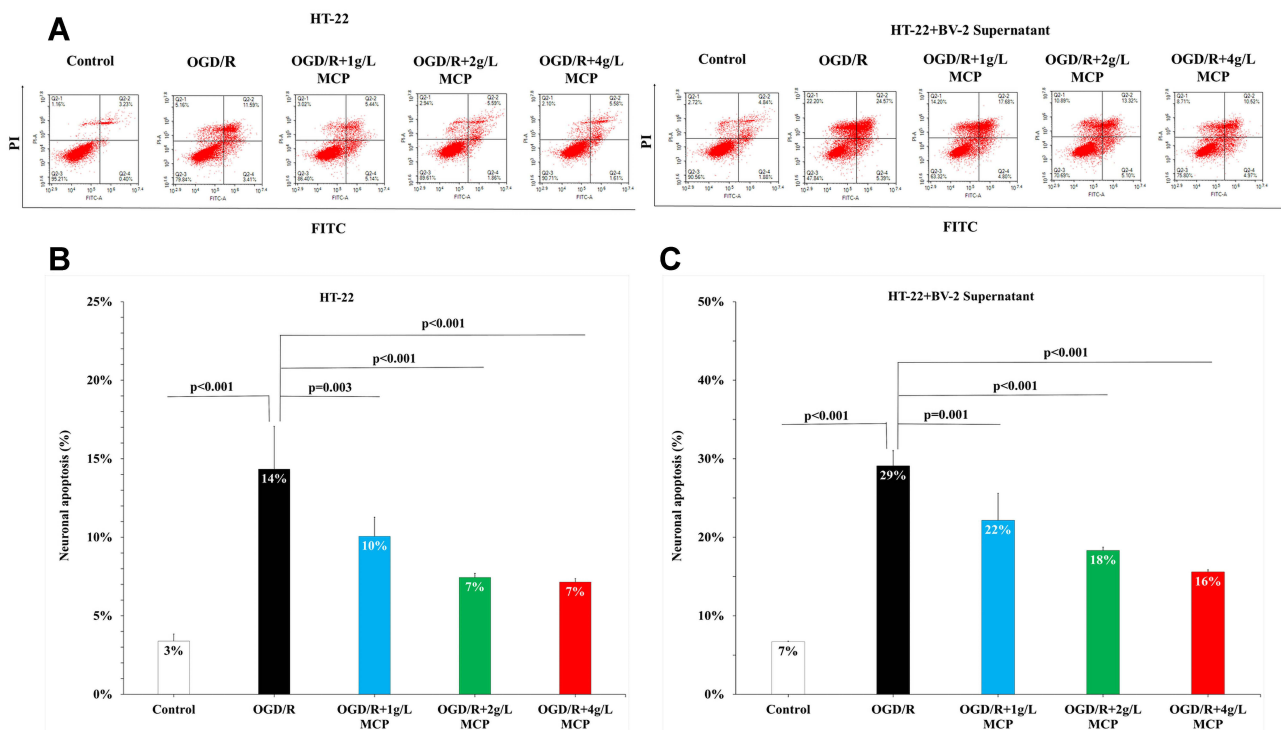


**Figure 5** MCP attenuated neuronal cell apoptosis in OGD/R model. (A) Neuronal cell (HT-22) apoptosis after OGD/R was assessed by flow cytometry. (B) Representative flow cytometry images of neuronal cell (HT-22) apoptosis. (C) Representative flow cytometry images of neuronal cell (HT-22) apoptosis, when co-cultured with supernatant of BV-2 cells. MCP indicates modified citrus pectin, OGD/R, oxygen-glucose deprivation/reperfusion. Data are mean  $\pm$  standard deviation, and  $n=5$  per group.

caused the activation of NLRP3 inflammasome in microglial cells, which was significantly inhibited by MCP (800 mg/kg/d) treatment vs vehicle ( $p = 0.006$ , Figure 6). Western blot analysis showed that MCP (400 mg/kg/d and 800 mg/kg/d) treatment significantly reduced the levels of NLRP3 ( $p < 0.001$  and  $p < 0.001$ ), cleaved caspase-1 ( $p = 0.001$  and  $p < 0.001$ ), and IL-1 $\beta$  ( $p = 0.006$  and  $p = 0.001$ ) at 1 day after reperfusion, compared with vehicle group (Figure 7). Similarly, MCP (1 g/L, 2 g/L, and 4 g/L) treatment significantly decreased the expression of NLRP3 ( $p < 0.001$ ,  $p < 0.001$ , and  $p < 0.001$ ), cleaved caspase-1 ( $p = 0.037$ ,  $p = 0.001$ , and  $p < 0.001$ ) and IL-1 $\beta$  ( $p = 0.005$ ,  $p = 0.001$ , and  $p < 0.001$ ) in the OGD/R BV-2 cells (Figure 8). The numerical data are shown in the [Supplementary Tables 11–13](#). The results suggested that MCP could reduce the inflammatory response following cerebral ischemia/reperfusion injury.

## MCP Inhibits the Activation of the Galectin-3/TLR4/NF- $\kappa$ B Signaling Pathway

In order to investigate the effect of MCP on the ischemia/reperfusion-induced galectin-3 expression, we performed the immunofluorescence staining and Western blot analyses. The results showed that cerebral ischemia/reperfusion caused the activation of galectin-3<sup>+</sup> cell in microglia, which was significantly inhibited by MCP (200 mg/kg/d, 400 mg/kg/d, and 800 mg/kg/d) treatment, compared with the vehicle group ( $p = 0.013$ ,  $p < 0.001$ , and  $p < 0.001$ , Figure 9). Compared with sham group, the expression of galectin-3 ( $p < 0.001$  and  $p < 0.001$ ), TLR4 ( $p = 0.017$  and  $p = 0.001$ ), and NF- $\kappa$ Bp65 ( $p = 0.006$  and  $p = 0.001$ ) were found to be elevated at 1 day after the MCAO/R operation, which was significantly inhibited by MCP (400 mg/kg/d and 800 mg/kg/d) (Figure 10). Similarly, 2 g/L and 4 g/L MCP significantly decreased the expression of galectin-3 ( $p < 0.001$  and  $p < 0.001$ ), TLR4 ( $p = 0.032$  and  $p = 0.004$ ), and NF- $\kappa$ Bp65 ( $p = 0.007$  and  $p < 0.001$ ) in the OGD/R BV-2 cells (Figure 11). The numerical data was shown in the [Supplementary Tables 14–16](#). The results suggested that MCP could blocked galectin-3 induced by cerebral ischemia/reperfusion injury and subsequently inhibited the followed activation of TLR4/NF- $\kappa$ B.

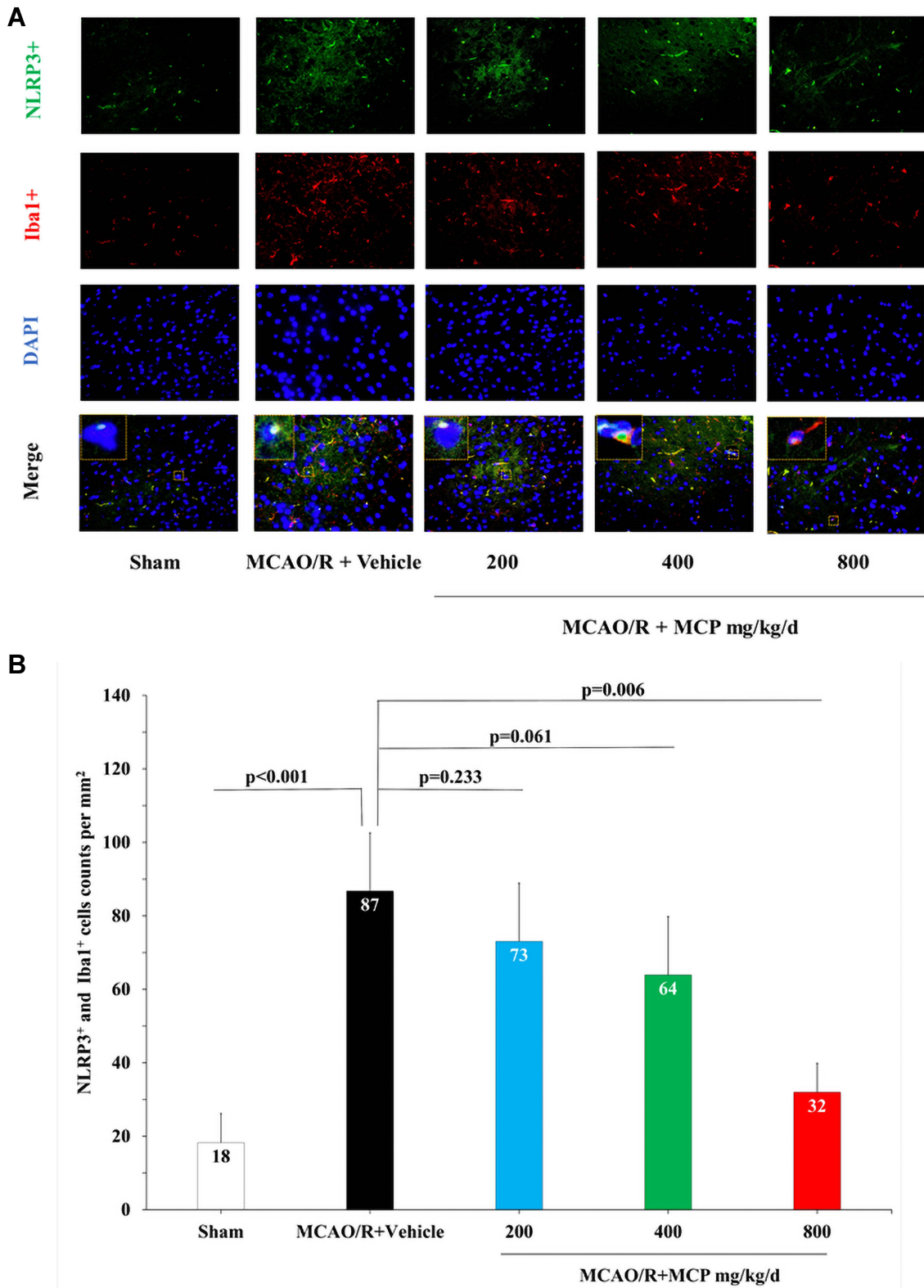


**Figure 6** MCP treatment reduced the co-expression of NLRP3 inflammasome and microglia in C57BL/6j mice at 1 day after MCAO/R operation. **(A)** Representative double immunofluorescence staining images of cerebral cortex with NLRP3 (green) and Iba1 (microglia, red), counterstained with DAPI,  $n=3$  per group, scale bar:  $50\mu\text{m}$ . **(B)** Quantification of merged cells in the ischemic penumbra. MCAO/R indicates middle cerebral artery occlusion/reperfusion; MCP, modified citrus pectin; NLRP3, NOD-like receptor 3. Data are mean  $\pm$  standard deviation, and  $n=3$  per group.

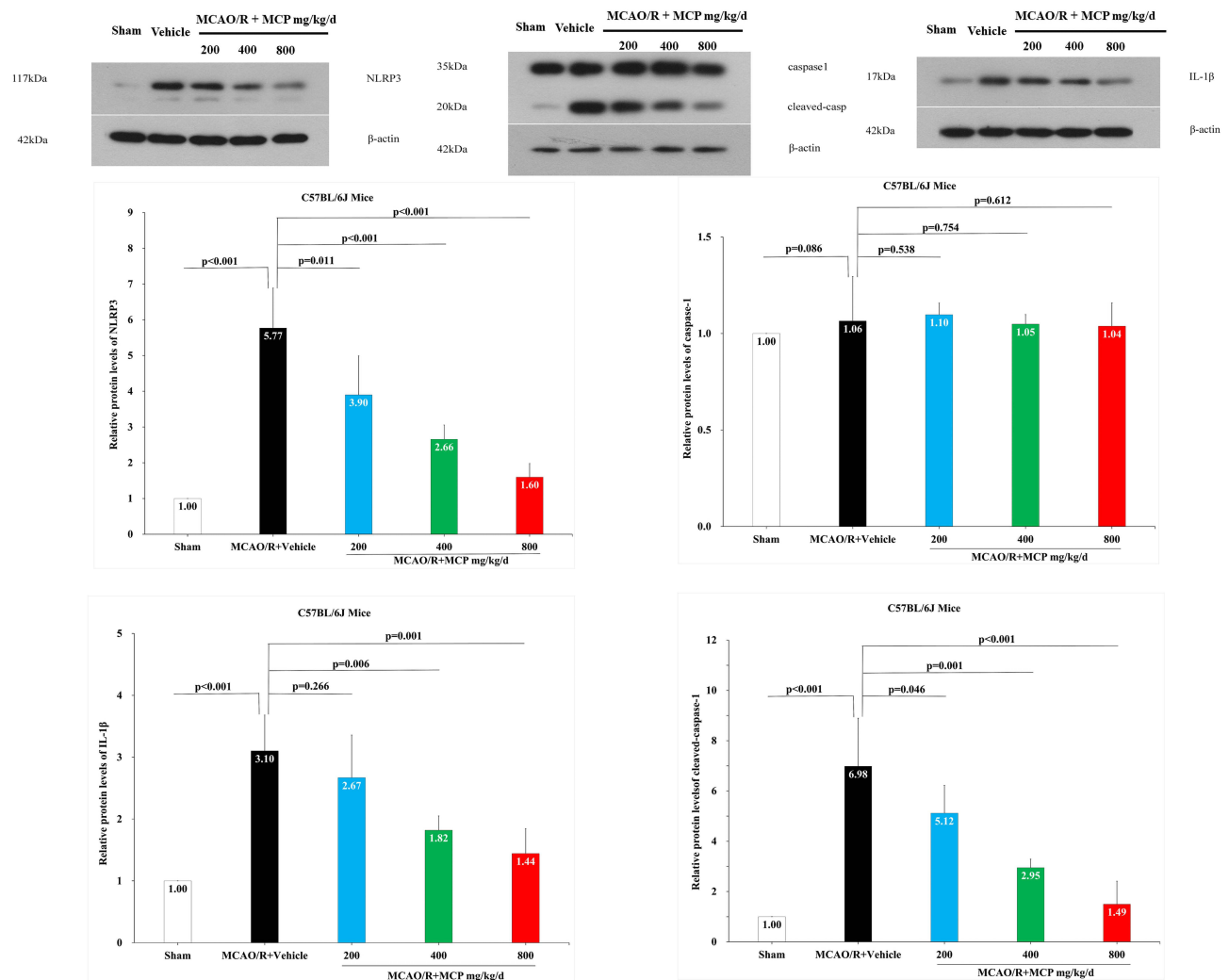


**Figure 7** The effects of MCP on NLRP3 inflammasome, cleaved-caspase-1/caspase-1, and IL-1β in cerebral cortex after MCAO/R injury. Western blot analysis showed that MCP treatment reduced the expression of NLRP3 inflammasome, cleaved-caspase-1, and IL-1β in C57BL/6J mice at 1 day after MCAO/R operation. Proteins had been normalized to β-actin. MCAO/R indicates middle cerebral artery occlusion/reperfusion; MCP, modified citrus pectin; NLRP3, NOD-like receptor 3. Data are mean ± standard deviation, and n=3 per group.

## Discussion

In the present study, for the first time, we identified that MCP had neuroprotective effects on cerebral ischemia/reperfusion injury: (1) MCP reduced infarction size, brain edema, neurons injury and apoptosis, and ameliorated neurological deficit in MCAO/R C57BL/6J mice; (2) MCP reduced injury and increased viability in OGD/R HT-22 cells. Furthermore, we found that the neuroprotective effect of MCP was mediated through inhibiting microglia and subsequent NLRP3 inflammasome activation via blocking galectin-3/TLR4/NF-κB signaling pathway.

Microglia, the resident macrophages of the brain, are activated rapidly in response to ischemic stroke.<sup>6</sup> Galectin-3, secreted from activated microglia, initiates inflammatory response in surrounding microglia, which results in brain injury following stroke.<sup>8,9</sup> In the present study, we found that cerebral ischemia/reperfusion injury initiated galectin-3 expression in microglia, which was inhibited by MCP treatment. Furthermore, our in vivo study showed that MCP ameliorated neurological deficit, infarct volume, and brain edema after cerebral ischemia/reperfusion injury. Thus, we inferred that MCP produced neuroprotective effects through inhibiting galectin-3 expression in microglia, which was further supported by our in vitro experiments. MCP administration markedly attenuated the increase of HT-22 cell viability, LDH activity, and apoptosis after HT-22 cells were co-cultured with the supernatant of BV-2 cells and then subjected to OGD/R, which was similar with the results in the previous studies.<sup>30,31</sup> Furthermore, we found that the effects of MCP on LDH

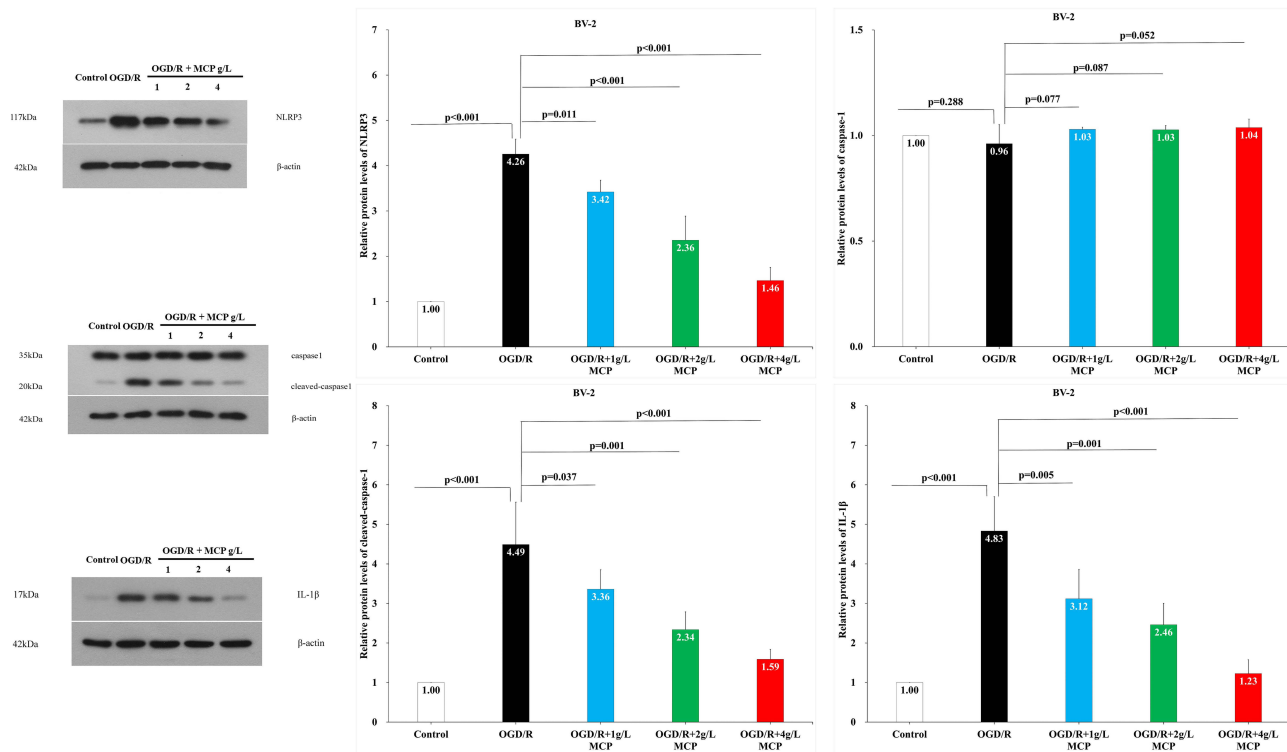


**Figure 8** The effects of MCP on NLRP3 inflammasome, cleaved-caspase-1/caspase-1, and IL-1β in microglial cells (BV-2) after OGD/R injury. Western blot analysis showed that MCP treatment reduced the expression of NLRP3 inflammasome, cleaved-caspase-1, and IL-1β in BV-2 cells after OGD/R operation. Proteins had been normalized to β-actin. OGD/R indicates oxygen-glucose deprivation/reperfusion; MCP, modified citrus pectin, NLRP3, NOD-like receptor 3. Data are mean ± standard deviation, and n=5 per group.

activity and apoptosis of HT-22 cells also remained present without co-culture with supernatant of BV-2 cells. The interesting phenomena warrants further investigations.

The inflammatory response after the initial ischemic insult is a key mechanism of secondary brain injury.<sup>6</sup> NLRP3 inflammasome activation has been demonstrated to significantly aggravate neuroinflammation and brain injury following experimental ischemic stroke.<sup>32–34</sup> Previous studies showed that galectin-3 was secreted from microglia after cerebral ischemic injury and triggered NF-κB activation by acting on the receptor TLR4 in the surrounding microglial cells,<sup>9</sup> which contributed to NLRP3 inflammasome activation.<sup>35</sup> Subsequently, activated NLRP3 inflammasome-induced procaspase-1 to caspase-1, in turn which converted pro-IL-1β to IL-1β.<sup>36,37</sup> Furthermore, neuroinflammation induced by activated microglia plays a key role in neuronal apoptosis through p53-mediated induction of proapoptotic Bcl-2 family members.<sup>38</sup> MCP, as galectin-3 inhibitor, has been used to suppress inflammatory response in several diseases.<sup>16,17,24,25</sup> Our current study further supported the anti-inflammatory effect of MCP in ischemic stroke, for example the inhibitory effect of MCP treatment on the expression of TLR4, NF-κBp65, and NLRP3 inflammasome-associated proteins in microglia. Thus, we speculated that the neuroprotective effects of MCP on anti-inflammation through blocking expression of galectin-3 was mediated by the axis of TLR4/NF-κB/NLRP3/cleaved-caspase-1/IL-1β in microglia (Figure 12). Nevertheless, some studies previously reported that IL-1β contributed to the proliferation of astrocytes and neurite growth,<sup>39,40</sup> which suggested that inflammatory cytokines may have beneficial effects on brain injury. Considering the dual effects of inflammatory response after stroke which may be time-dependent,<sup>12</sup> the neuroprotective time window of MCP through inhibiting galectin-3 induced inflammation warranted investigation in the future.

## Study Limitations

It is worth mentioning that there are some limitations in the present study. First, due to lack of cells double-labeled with both TUNEL and NeuN in the staining assay, positive cells labeled with only TUNEL could not accurately represent the apoptosis of neurons. Second, there was a lack of dynamic change of NLRP3 inflammasome-associated proteins. For

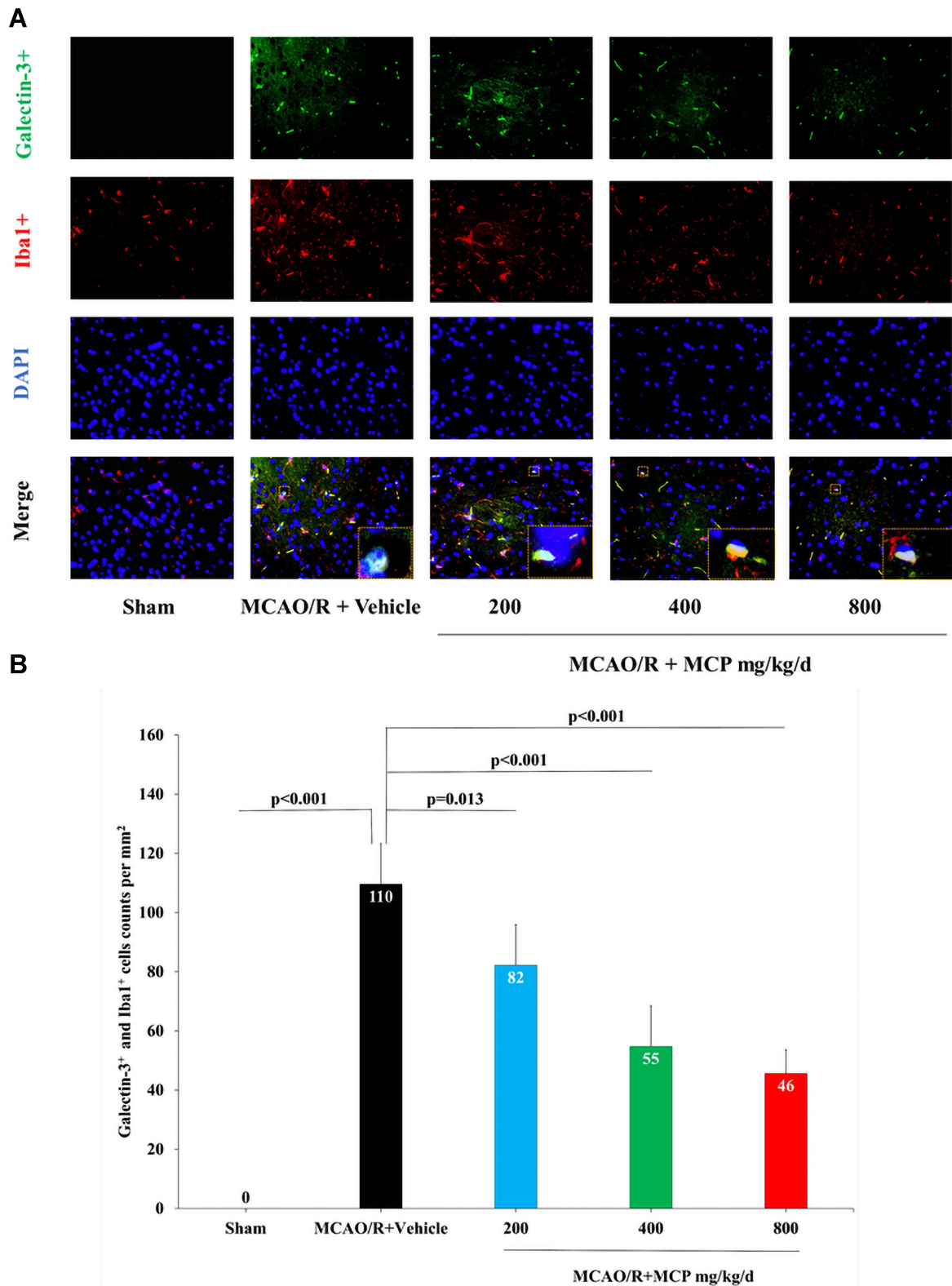


**Figure 9** MCP treatment reduced the co-expression of galectin-3 and microglia, and TLR4, NF- $\kappa$ Bp65 in C57BL/6J mice at 1 day after MCAO/R operation. **(A)** Representative double immunofluorescence staining images of cerebral cortex with galectin-3 (green) and Iba1 (microglia, red), counterstained with DAPI,  $n=3$  per group, scale bar: 50 $\mu$ m. **(B)** Quantification of merged cells in the ischemic penumbra. Data are mean  $\pm$  standard deviation.

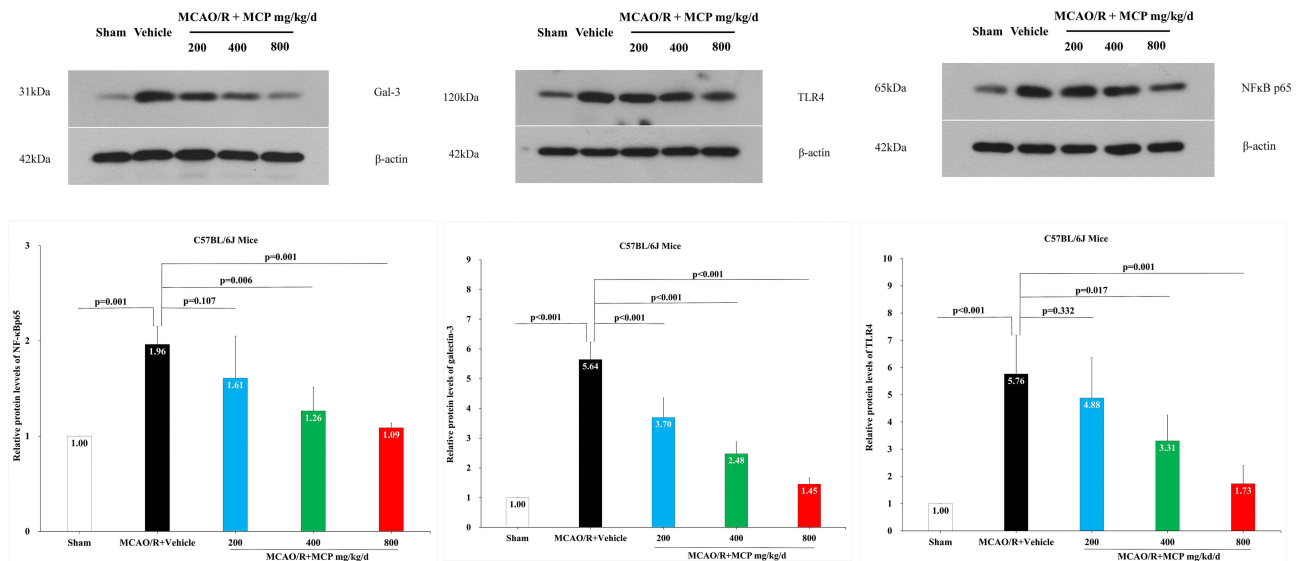


**Figure 10** The effects of MCP on TLR4, NF-κBp65, and galectin-3 in cerebral cortex after MCAO/R injury. Western blot analysis showed that MCP treatment reduced the expression of TLR4, NF-κBp65, and galectin-3 in C57BL/6J mice at 1 day after MCAO/R operation. Proteins had been normalized to β-actin. MCAO/R indicates middle cerebral artery occlusion/reperfusion; MCP, modified citrus pectin. Data are mean ± standard deviation, and n=3 per group.

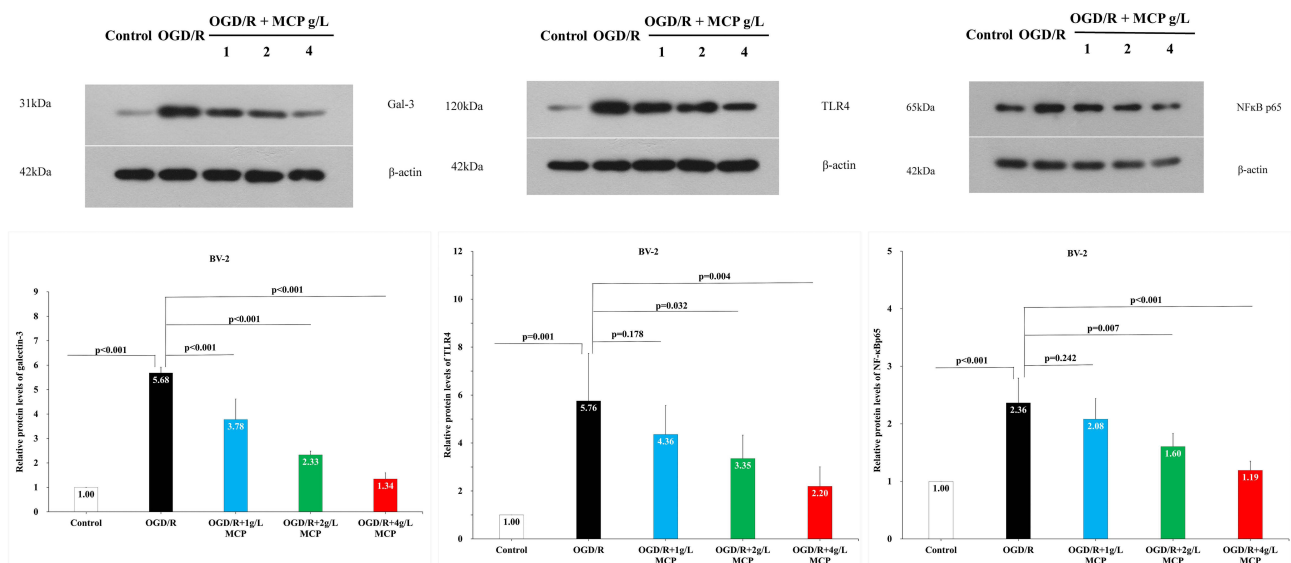


**Figure 11** The effects of MCP on TLR4, NF-κBp65, and galectin-3 in microglial cells (BV-2) after OGD/R injury. Western blot analysis showed that MCP treatment reduced the expression of TLR4, NF-κBp65, and galectin-3 in BV-2 cells after OGD/R operation. Proteins had been normalized to β-actin. OGD/R indicates oxygen-glucose deprivation/reperfusion; MCP, modified citrus pectin. Data are mean ± standard deviation, and n=5 per group.

example, we did not detect the levels of NLRP3 inflammasome-associated proteins before and after MCP treatment, which could be helpful to better illustrate the association between protein changes and MCP treatment. Third, we only determined neurologic deficit scoring at 1 day after MCAO/R operation; thus, it is unclear as to the long-term neuroprotective effect. Fourth, the current study did not investigate whether the effects of MCP were mediated by galectin-3, which deserved to be determined. Last, given the difference of the pharmacological dynamics between in vitro and in vivo experiments, it is better to measure the concentration of MCP in different times, which was not performed in the current study. The current study showed that MCP treatment could improve neurological deficit scoring of MCAO/R mice after administering daily for 5 days ([Supplementary Figure 2](#)), and we inferred that the neuroprotection of MCP may be due to the effect of its accumulating doses over days. In the current study, pre-administration of MCP was used to

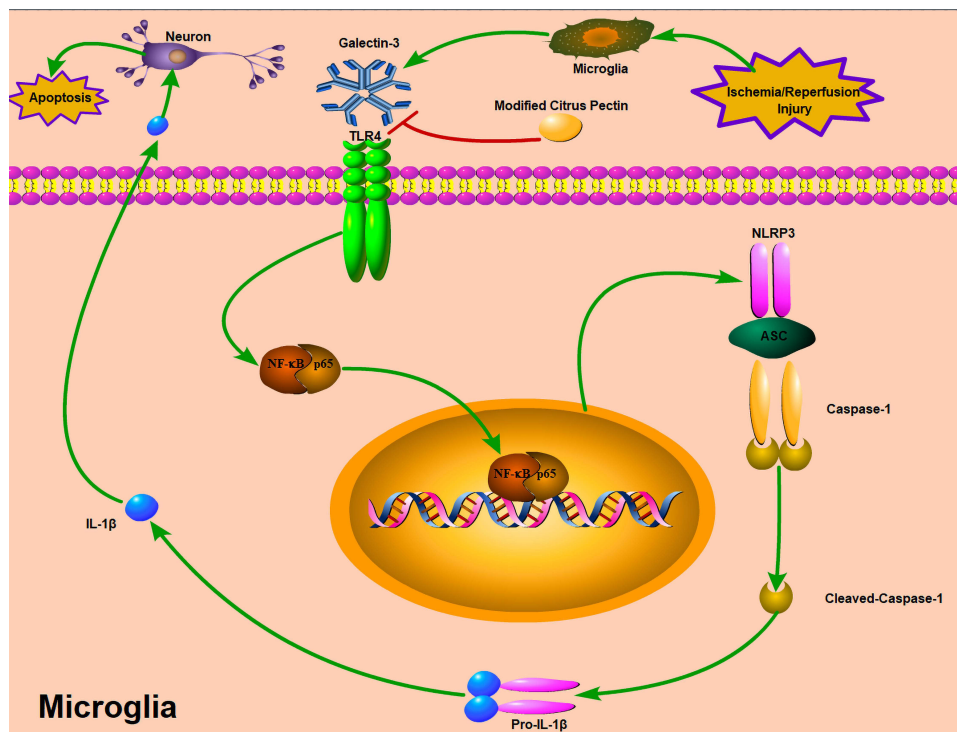


**Figure 12** Potential mechanisms by which MCP protects against cerebral ischemia/reperfusion injury. MCP indicates modified citrus pectin. Cerebral ischemic insult may promote the expression of galectin-3 in microglia, and then trigger the activation of NLRP3 inflammasome in microglia through TLR4/NF- $\kappa$ B signaling pathway, which converts caspase-1 into cleaved-caspase-1. Cleaved-caspase-1 further converts pro-IL-1 $\beta$  into IL-1 $\beta$ , which is then secreted into the extracellular space and contributes to secondary inflammatory response. The neuroprotective effects of MCP on anti-inflammation through blocking expression of galectin-3 was mediated by the axis of TLR4/NF- $\kappa$ B/NLRP3/cleaved-caspase-1/IL-1 $\beta$  in microglia.

assess the neuroprotective effect of MCP, which is not a clinically viable strategy. Thus, it will be worth further exploring the neuroprotection in cerebral ischemic/reperfusion injury when MCP administration after stroke onset.

## Conclusions

In summary, this is the first report that MCP, as a blocker of galectin-3, may exert neuroprotective effects on cerebral ischemia/reperfusion injury, probably through inhibiting the activation of NLRP3 inflammasome via TLR4/NF- $\kappa$ B signaling pathway. Given that the routine uses of MCP in several diseases, these findings pave the way for translational clinical trial on stroke.

## Data Sharing Statement

The datasets used and analyzed during the current study are available from the corresponding author on reasonable request.

## Ethics Approval

The Animal Ethics Review Committee of General Hospital of Northern Theater Command approved all procedures. The study followed the laboratory animal-guideline for ethical review of animal welfare in China.

## Acknowledgments

We thank Dai-Chao Ma, Zhao-Shi Bai, Zi-Nv Zhang, Yi-Na Zhang, Ming-Yue Liu and Yue Yang for providing technical assistance.

## Author Contributions

All authors made a significant contribution to the work reported, whether that is in the conception, study design, execution, acquisition of data, analysis and interpretation, or in all these areas; took part in drafting, revising or critically reviewing the article; gave final approval of the version to be published; have agreed on the journal to which the article has been submitted; and agreed to be accountable for all aspects of the work.

## Funding

The study was funded by grants from the National Natural Science Foundation of the People's Republic of China (8207147).

## Disclosure

The authors have no competing interests to declare in this work.

## References

- Campbell BCV, Khatri P. Stroke. *Lancet*. 2020;396(10244):129–142. doi:10.1016/S0140-6736(20)31179-X
- Wahlgren N, Ahmed N, Dávalos A, et al. Thrombolysis with alteplase for acute ischaemic stroke in the Safe Implementation of Thrombolysis in Stroke-Monitoring Study (SITS-MOST): an observational study. *Lancet*. 2007;369(9558):275–282. doi:10.1016/S0140-6736(07)60149-4
- Yu WM, Abdul-Rahim AH, Cameron AC, et al. The incidence and associated factors of early neurological deterioration after thrombolysis: results from SITS registry. *Stroke*. 2020;51(9):2705–2714. doi:10.1161/STROKEAHA.119.028287
- Shi K, Zou M, Jia D-M, et al. tPA mobilizes immune cells that exacerbate hemorrhagic transformation in stroke. *Circ Res*. 2021;128(1):62–75. doi:10.1161/CIRCRESAHA.120.317596
- Petrovic-Djergovic D, Goonewardena SN, Pinsky DJ. Inflammatory disequilibrium in stroke. *Circ Res*. 2016;119(1):142–158. doi:10.1161/CIRCRESAHA.116.308022
- Jin R, Yang G, Li G. Inflammatory mechanisms in ischemic stroke: role of inflammatory cells. *J Leukoc Biol*. 2010;87(5):779–789. doi:10.1189/jlb.1109766
- Hernández IH, Villa-González M, Martín G, Soto M, Pérez-álvarez MJ. Glial cells as therapeutic approaches in brain ischemia-reperfusion injury. *Cells*. 2021;10(7):1639. doi:10.3390/cells10071639
- Rahimian R, Béland LC, Kriz J. Galectin-3: mediator of microglia responses in injured brain. *Drug Discov Today*. 2018;23(2):375–381. doi:10.1016/j.drudis.2017.11.004
- Burguillos MA, Svensson M, Schulte T, et al. Microglia-secreted galectin-3 acts as a toll-like receptor 4 ligand and contributes to microglial activation. *Cell Rep*. 2015;10(9):1626–1638. doi:10.1016/j.celrep.2015.02.012
- Venkatraman A, Hardas S, Patel N, Singh Bajaj N, Arora G, Arora P. Galectin-3: an emerging biomarker in stroke and cerebrovascular diseases. *Eur J Neurol*. 2018;25(2):238–246. doi:10.1111/ene.13496
- Kopitar-Jerala N. Innate immune response in brain, NF-Kappa B SIGNALING AND Cystatins. *Front Mol Neurosci*. 2015;8:73. doi:10.3389/fnmol.2015.00073
- Xu S, Lu J, Shao A, Zhang JH, Zhang J. Glial cells: role of the immune response in ischemic stroke. *Front Immunol*. 2020;11:294. doi:10.3389/fimmu.2020.00294
- Lau ES, Liu E, Paniagua SM, et al. Galectin-3 inhibition with modified citrus pectin in hypertension. *JACC Basic Transl Sci*. 2021;6(1):12–21. doi:10.1016/j.jacbts.2020.10.006
- Xu GR, Zhang C, Yang HX, et al. Modified citrus pectin ameliorates myocardial fibrosis and inflammation via suppressing galectin-3 and TLR4/MyD88/NF-κB signaling pathway. *Biomed Pharmacother*. 2020;126:110071. doi:10.1016/j.biopha.2020.110071
- Yin Q, Chen J, Ma S, et al. Pharmacological inhibition of Galectin-3 ameliorates diabetes-associated cognitive impairment, oxidative stress and neuroinflammation in vivo and in vitro. *J Inflamm Res*. 2020;13:533–542. doi:10.2147/JIR.S273858
- Ibarrola J, Matilla L, Martínez-Martínez E, et al. Myocardial injury after ischemia/reperfusion is attenuated by pharmacological Galectin-3 inhibition. *Sci Rep*. 2019;9(1):9607. doi:10.1038/s41598-019-46119-6
- Martínez-Martínez E, Calvier L, Fernández-Celis A, et al. Galectin-3 blockade inhibits cardiac inflammation and fibrosis in experimental hyperaldosteronism and hypertension. *Hypertension*. 2015;66(4):767–775. doi:10.1161/HYPERTENSIONAHA.115.05876
- Dong H, Wang ZH, Zhang N, Liu SD, Zhao JJ, Liu SY. Serum Galectin-3 level, not Galectin-1, is associated with the clinical feature and outcome in patients with acute ischemic stroke. *Oncotarget*. 2017;8(65):109752–109761. doi:10.18632/oncotarget.18211
- Wang A, Zhong C, Zhu Z, et al. Serum Galectin-3 and poor outcomes among patients with acute ischemic stroke. *Stroke*. 2018;49(1):211–214. doi:10.1161/STROKEAHA.117.019084
- Zeng N, Wang A, Zhong C, et al. Association of serum galectin-3 with risks of death and vascular events in acute ischaemic stroke patients: the role of hyperglycemia. *Eur J Neurol*. 2019;26(3):415–421. doi:10.1111/ene.13856
- Zeng N, Wang A, Xu T, et al. Co-effect of serum Galectin-3 and high-density lipoprotein cholesterol on the prognosis of acute ischemic stroke. *J Stroke Cerebrovasc Dis*. 2019;28(7):1879–1885. doi:10.1016/j.jstrokecerebrovasdis.2019.04.007
- Hansen C, Sastre C, Wolcott Z, Bevers MB, Kimberly WT. Time-dependent, dynamic prediction of fatty acid-binding protein 4, Galectin-3, and soluble ST2 measurement with poor outcome after acute stroke. *Int J Stroke*. 2021;16(6):660–668. doi:10.1177/1747493020971166
- Zhuang JJ, Zhou L, Zheng YH, Ding YS. The serum galectin-3 levels are associated with the severity and prognosis of ischemic stroke. *Aging*. 2021;13(5):7454–7464. doi:10.18632/aging.202610
- Percie du Sert N, Hurst V, Ahluwalia A, et al. The ARRIVE guidelines 2.0: updated guidelines for reporting animal research. *J Cereb Blood Flow Metab*. 2020;40(9):1769–1777. doi:10.1177/0271678X20943823



25. Vahidy F, Schäbitz WR, Fisher M, Aronowski J. Reporting standards for preclinical studies of stroke therapy. *Stroke*. 2016;47(10):2435–2438. doi:10.1161/STROKEAHA.116.013643
26. Wu LR, Liu L, Xiong XY, et al. Vinpocetine alleviate cerebral ischemia/reperfusion injury by down-regulating TLR4/MyD88/NF-κB signaling. *Oncotarget*. 2017;8(46):80315–80324. doi:10.18632/oncotarget.20699
27. Longa EZ, Weinstein PR, Carlson S, Cummins R. Reversible middle cerebral artery occlusion without craniectomy in rats. *Stroke*. 1989;20(1):84–91. doi:10.1161/01.str.20.1.84
28. Hatashita S, Hoff JT, Salamat SM. Ischemic brain edema and the osmotic gradient between blood and brain. *J Cereb Blood Flow Metab*. 1988;8(4):552–559. doi:10.1038/jcbfm.1988.96
29. Qin X, Sun ZQ, Zhang XW, Dai XJ, Mao SS, Zhang YM. TLR4 signaling is involved in the protective effect of propofol in BV2 microglia against OGD/reoxygenation. *J Physiol Biochem*. 2013;69(4):707–718. doi:10.1007/s13105-013-0247-6
30. Zhang Z, Qin P, Deng Y, et al. The novel estrogenic receptor GPR30 alleviates ischemic injury by inhibiting TLR4-mediated microglial inflammation. *J Neuroinflammation*. 2018;15(1):206. doi:10.1186/s12974-018-1246-x
31. Ma Z, Zhang Z, Bai F, Jiang T, Yan C, Wang Q. Electroacupuncture pretreatment alleviates cerebral ischemic injury through α7 nicotinic acetylcholine receptor-mediated phenotypic conversion of microglia. *Front Cell Neurosci*. 2019;13:537. doi:10.3389/fncel.2019.00537
32. Ma C, Liu S, Zhang S, et al. Evidence and perspective for the role of the NLRP3 inflammasome signaling pathway in ischemic stroke and its therapeutic potential (Review). *Int J Mol Med*. 2018;42(6):2979–2990. doi:10.3892/ijmm.2018.3911
33. Hong P, Gu RN, Li FX, et al. NLRP3 inflammasome as a potential treatment in ischemic stroke concomitant with diabetes. *J Neuroinflammation*. 2019;16(1):121. doi:10.1186/s12974-019-1498-0
34. Yang G, Jang JH, Kim SW, et al. Sweroside prevents non-alcoholic steatohepatitis by suppressing activation of the NLRP3 inflammasome. *Int J Mol Sci*. 2020;21(8):2790. doi:10.3390/ijms21082790
35. Fann DY, Lee SY, Manzanero S, Chunduri P, Sobey CG, Arumugam TV. Pathogenesis of acute stroke and the role of inflammasomes. *Ageing Res Rev*. 2013;12(4):941–966. doi:10.1016/j.arr.2013.09.004
36. Alishahi M, Farzaneh M, Ghaedrahmati F, Nejabatdoust A, Sarkaki A, Khoshnam SE. NLRP3 inflammasome in ischemic stroke: as possible therapeutic target. *Int J Stroke*. 2019;14(6):574–591. doi:10.1177/1747493019841242
37. Zhang Q, Chen C, Lü J, et al. Cell cycle inhibition attenuates microglial proliferation and production of IL-1β, MIP-1α, and NO after focal cerebral ischemia in the rat. *Glia*. 2009;57(8):908–920. doi:10.1002/glia.20816
38. Guadagno J, Swan P, Shaikh R, Cregan SP. Microglia-derived IL-1β triggers p53-mediated cell cycle arrest and apoptosis in neural precursor cells. *Cell Death Dis*. 2015;6(6):e1779. doi:10.1038/cddis.2015.151
39. Rühl A, Franzke S, Stremmel W. IL-1β and IL-10 have dual effects on enteric glial cell proliferation. *Neurogastroenterol Motil*. 2001;13(1):89–94. doi:10.1046/j.1365-2982.2001.00245.x
40. Boato F, Hechler D, Rosenberger K, et al. Interleukin-1 beta and neurotrophin-3 synergistically promote neurite growth in vitro. *J Neuroinflammation*. 2011;8(1):183. doi:10.1186/1742-2094-8-183

## Publish your work in this journal

The Journal of Inflammation Research is an international, peer-reviewed open-access journal that welcomes laboratory and clinical findings on the molecular basis, cell biology and pharmacology of inflammation including original research, reviews, symposium reports, hypothesis formation and commentaries on: acute/chronic inflammation; mediators of inflammation; cellular processes; molecular mechanisms; pharmacology and novel anti-inflammatory drugs; clinical conditions involving inflammation. The manuscript management system is completely online and includes a very quick and fair peer-review system. Visit <http://www.dovepress.com/testimonials.php> to read real quotes from published authors.

Submit your manuscript here: <https://www.dovepress.com/journal-of-inflammation-research-journal>